Open Access **Baghdad Science Journal** **P-ISSN: 2078-8665**
Published Online First: November 2021 **2022, 19(3): 660-669** **E-ISSN: 2411-7986**

DOI: http://dx.doi.org/10.21123/bsj.2022.19.3.0660

Preparation and study of the Structural, Morphological and Optical properties of pure Tin Oxide Nanoparticle doped with Cu

Duha S. Shaker* ***Nada K. Abass*** ***Ruqayah A. Ulwali***

Department of Physics, College of Science for Women, University of Baghdad, Baghdad, Iraq.
Corresponding author: doha.saad1204a@csw.uobaghdad.edu.iq, nadabbs@yahoo.com , ruqayah_phy@yahoo.com
ORCID ID: https://orcid.org/0000-0002-7746-663X, https://orcid.org/0000-0001-8573-4174, https://orcid.org/0000-0003-3252-7483

Received 22/4/2021, Accepted 7/7/2021, Published Online First 20/11/2021 Published 1/6/2022

Abstract:

In this study, pure SnO_2 Nanoparticles doped with Cu were synthesized by a chemical precipitation method. Using $SnCl_2.2H_2O$, $CuCl_2.2H_2O$ as raw materials, the materials were annealed at 550°C for 3 hours in order to improve crystallization. The XRD results showed that the samples crystallized in the tetragonal rutile type SnO_2 stage. As the average SnO_2 crystal size is pure 9nm and varies with the change of Cu doping (0.5%, 1%, 1.5%, 2%, 2.5%, 3%),(8.35, 8.36, 8.67, 9 ,7, 8.86)nm respectively an increase in crystal size to 2.5% decreases at this rate and that the crystal of SnO_2 does not change with the introduction of Cu, and SEM results of the pure and doped confirmed that the particle size is within the range (25-56)nm within the nanosize. UV-Vis studies of reflection spectroscopy revealed that energy of band gap increased with increasing doping ratios (4.33,4.18 ,4.21, 4.21 4.23,4.35) ev For pure and doped with Cu (0.5%, 1%, 1.5%, 2%, 2.5%, 3%) respectively. Results of AFM show roughness rate, SPM and grain size of pure samples doped with Cu where the roughness rate of SnO_2 is (3.04, 25,27,16,41.8,23.6,25.2) nm and average diameter is (98.9, 72.56 ,92.91, 88.38, 76.79, 70.94, 71.21) nm for pure and doped with Copper (0.5%, 1%, 1.5%, 2%, 2.5%, 3%) respectively.

Keywords: Cu Doped SnO_2 Nanoparticles، Precipitation method، UV and particle size analyzer, SEM، Tin oxide.

Introduction:

In recent years, nanotechnology has become one of the most priority areas in chemistry, physics and biology .The basis of nanotechnology is that the particle size is less than 100nm and thus we will get a new behavior that depends on the size, it has been observed that the conductivity melting temperature , mechanical and electrical properties، change when the particles become smaller than Critical size [1] .Thus, stronger, lighter, and stiffer materials will be produced due to two important factors: Increased surface area , Quantum effect.

The impetus that caused this technology to advance so rapidly is the development of devices such as the Scanning electron microscope; the Transmission electron microscope; the Atomic force microscope and other devices[2]. The physical and chemical properties of nanomaterials differ compared to bulk in these materials, as the presence of atoms or impurities to modify the electronic, optical and magnetic properties of bulk semiconductors[3]. The researchers have been interested in metal oxide semiconductors due to their unique physical and chemical properties، these properties are increased and improved by doping other ingredients [4-6]. It is like these oxides.((ZnO, TiO_2, WO_3, CeO_3 and SnO_2 etc [7,8]

Tin oxide is an important material because it has a high degree of transparency in the visible spectrum. It has a strong chemical and physical interaction with absorbent species. It also has a low operating temperature. Strongly thermally stable in the air up to 500°C [9] , Tin has two types of oxides; stannous oxide (**SnO** – romarchite) and stannic oxide (**SnO_2** – cassiterite) [10] .

Tin oxide (SnO_2) is one of the (n-type) metallic semiconductors that has a wide gap (3.6ev) in room temperature, and its excellent properties make it a suitable material for many applications, in transparent electrodes, solar cells, gas-sensing photocatalysts, photoelectric devices[11,12]

One of the influences that affect the performance of the sensors is the increase in the surface area , as attention has been paid to preparing crystalline materials with a large surface area where the properties of crystalline materials are very sensitive on the surface of atomic structures, especially applications such as solar cells and gas sensors [13-15]. Oxide nanoparticles can be prepared by both Physical and Chemical methods. Chemical methods are better because they are easy to use and inexpensive Therefore, nanoparticles were synthesized by chemical methods[16].

One of the inexpensive chemical methods that aims to create high-quality nanoparticles at low temperatures and not the need for a special atmosphere is the method of chemical precipitation, as in this study the pure and doped nanoparticles of tin oxide were synthesized and manufactured by this method [17].

There are many processes for creating SnO_2 nanoparticles such as hydrothermal methods, chemical vapor deposition, Sol –gel method[18,19] ; However, in this study, SnO_2 pure nanoparticles were synthesized by the chemical precipitation method as well as the doped copper element.

Copper is a reddish-colored metal whose color and properties change when it unites with other elements in the form of different compounds that exist in several forms, single or combined such as oxides and it is a soft malleable substance that interacts chemically or physically with the external source, which is the atmosphere that creates rust. It has high electrical and thermal conductivity. The metal is the most electric and thermal conductor after silver[20,21] .

This study aims to prepare the nanomaterial from pure SnO_2 doped with Cu by the method of chemical precipitation, as this nanomaterial has wide applications including sensitizing gases such as (CO_2, NH_3), data storage, in solar cells, anti-bacterial applications.

Materials and Methods:

Materials:

$SnCl_2.2H_2O$ (Stannous chloride dehydrate Supplier Company CDH- Indian) , $CuCl_2.2H_2O$ (Cupric chloride dehydrate Supplier Company CDH- Indian), Triton X-100 ($C_{14}H_{22}O(C_2H_4O)_n$) Company Thomas baker as a surfactant , ammonia (NH_3) Company Thomas baker as precipitator were used to prepare pure Tin Oxide Nanoparticle and doped with Cu.

Preparation of pure Tin Oxide Nanoparticle and doped with Cu

Pure SnO_2 and doped with Cu nanoparticle were prepared by chemical precipitation method. 2g of tin chloride ($SnCl_2.2H_2O$) was used and dissolved in 100ml deionized water to make a 0.1M solution where molarity is given by relation 1 [22]:

$$M=\frac{W}{m.wt}\times\frac{1000}{V} \quad \text{.....1}$$

V: The volume of deionized water، W: the weight ، $m.wt$: Molecular weight

The resulting solution was placed on the stirring device (1500 rpm) for homogenization for 30 minutes, then a surfactant (Triton X-100) was added. We notice that the solution changed its color to white, then we add ammonia by distillation to the resulting solution while it is on the stirring device until it reaches the pH = 8, the color of the final product became milky. Then the solution was filtered and washed more than once in a centrifuge to separate unwanted materials, the product was left at room temperature for two days to dry out. After drying, the product was collected which was reddish-brown and annealed at 550 °C for 3 hours, and the final product was yellow in color after annealing. SnO_2 doped with Cu was prepared in the same way but by adding (0.5, 1, 1.5,2, 2.5, and 3) %wt of $CuCl_2.2H_2O$ into $SnCl_2.2H_2O$ and that is through the following relationship 2 [23]:

$$\%dopants=\frac{M\ (Cu\ Cl2\ .2H2O)\ molarity}{M\ (Cu\ Cl2\ .2H2O)+M\ SnCl2.2H2O} \quad \text{.....2}$$

M $(Cu\ Cl2\ .2H2O)\ molarity$: The molar concentration doped $CuCl_2.2H_2O$(X) , % dopants : doped concentrations (0.5, 1, 1.5,2, 2.5, and 3) %wt , $M\ SnCl2.2H2O$: 0.1 M

The color of the solution changed to green, the intensity of the color changed with the concentration, annealing the concentrations at 550°C for 3 hours in the presence of air.

Characterization

The X-ray diffraction (XRD) pattern of pure SnO_2 and doped with Cu nanoparticles were recorded by a system Siemens model D500 using CuKα,λ=0.154 nm. The particle morphology and size were examined by scanning electron microscopy (SEM) ZEISS model SigmaVP with a magnification of 50.00KX and (EDX) Oxford instruments UK. Optical properties were analyzed by means of ultraviolet diffusion. The Reflection Spectroscopy with UV-VIS (Shimadzu) was done within the wavelength range of 280 nm-900nm. The AFM showed the morphology of the SnO_2 NPs, and the average grain size was found by the cumulative distribution plot.

Results and Discussion:

XRD analysis

Fig1 shows the XRD pattern of pure SnO_2 and doped with Cu nanoparticles with concentrations of (0.5%, 1%, 1.5%, 2%, 2.5% and 3%)w% respectively and annealing at 550°C for 3 hours. All samples were identified as tetragonal rutile, and the results are in agreement with JCPDS standard card No. (96-900-9083) where the diffraction peaks coincide with the standard data from (110), (101), (211) and the most obvious peak is (110). There are no identical peaks for Cu .The results match those of the researchers Sagadevan et al. [24]. and this leads to the conclusion that there are two types of doped SnO_2 with Cu: substitutive and interstitial. In this case, some ions are replaced by Sn^+ with a Cu^+ ion based on similar radius Cu, Sn (0.73,0.69)Å [25], respectively .The average grain size of the nanoparticles were calculated based on Scherrer's eq.3 [26] :

$$d = \frac{\kappa\lambda}{\beta cos\theta} \quad \ldots\ldots\ldots\ldots\ldots 3$$

d : is the mean crystalline size, κ is the constant 0.89, λ is the wavelength of the incident beam (λ=1.5418Å) Cukα, β is the full width at half maximum,θ is the Bragg diffraction angle (in degrees). The crystal size of pure SnO_2 is 9.9nm, but when doped with Cu, it becomes less than 8.35nm. The reason for this is the quantum confinement effect. When increasing the doping led to an increase in the crystal size because the radius of Cu greater than Sn increased the G.S, but at 2.5% the size decreased. The reason for this is that there were defects in the system that led to the deflected of the diffraction angle of 2θ so the distance between the atomic levels decreased (d) according to Bragg's law (nλ=2d sinθ) [27] as a result of which increased FWHM(β) according to Scherrer eq.3 at 2.5% the crystal size decreases ,Tab. 2 shows the lattice constants for pure SnO_2 nanoparticles and doped with Cu , which can be calculated using the eq. 4:

$$\frac{1}{d^2} = \frac{h^2+k^2}{a^2} + \frac{l^2}{c^2} \quad \ldots\ldots\ldots\ldots\ldots 4$$

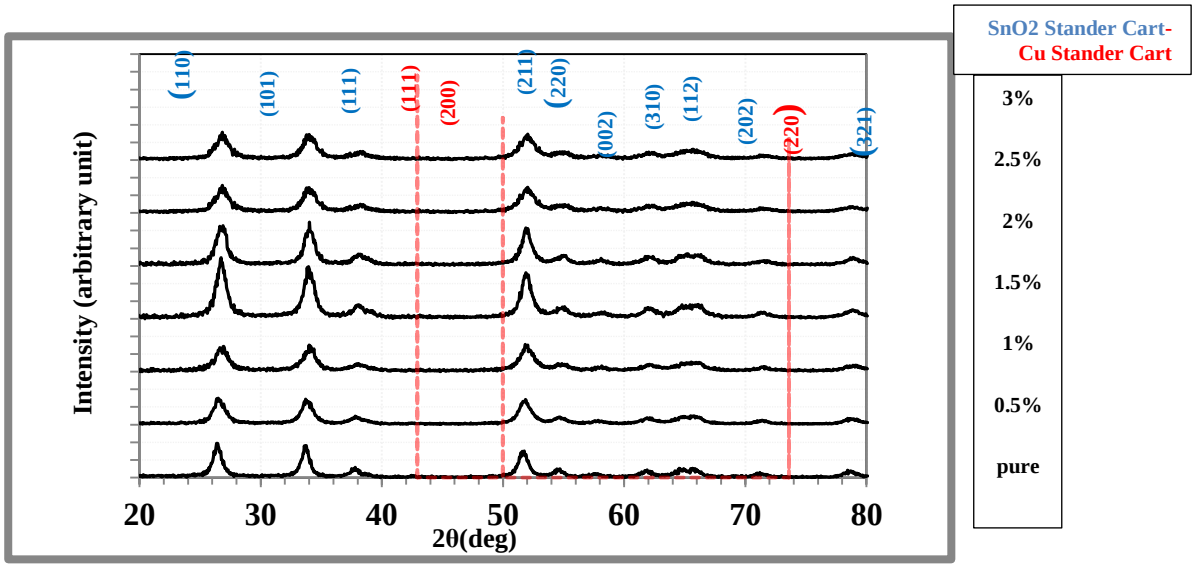

Figure. 1 X-ray diffraction pattern of pure Sno_2 nanoparticles doped with concentrations (0.5, 1, 1.5, 2, 2.5, and 3) %wt of Cu.

Table 1. Crystal Size of the pure SnO_2 nanoparticles doped with concentrations (0.5, 1, 1.5, 2, 2.5, and 3)%wt of Cu.

Cu%	G.S(nm)
0	9.97
0.5	8.35
1	8.36
1.5	8.67
2	9
2.5	7
3	8.86

Table 2. Lattice constants for pure SnO_2 nanoparticles doped with concentrations (0.5, 1, 1.5, 2, 2.5, and 3) %wt of Cu

Cu%	a (Å)	c (Å)
0	4.76956	3.19340
0.5	4.76368	3.20314
1	4.73508	3.15179
1.5	4.71245	3.18415
2	4.69005	3.18247
2.5	4.70066	3.18680
3	4.70582	3.18115

SEM scan results

Fig.2 shows the SEM images of the pure SnO_2 and doped with Cu nanoparticles at proportions (0.5%, 1%, 1.5%, 2%, 2.5%, 3%) respectively prepared by chemical precipitation method.

Since the SEM images give clarity about the surface morphology and the average particle size shown in this figure ranges from 25nm to 56nm, these nanoparticles contain spherical shapes with sizes smaller than 100 nm (Sarmah et al.) [28]. The particles were agglomerated, and the reason for this was due to the adhesion of particles to each other by the forces of Vander Waals, and the reason was due to the formation of covalent or metallic bonds that could not be separated easily [29]. Its reason is that during the process of initial contact of water molecules with SnO2, these agglomerations occur and lead to the trapping of water between the particles. Also, the electric charges between the particles affect the agglomeration of the particles. The mutual electrostatic repulsion force is produced between the neighboring particles [30] It can be noted that crystallite size ≤ grain size ≤ and particle size (i.e. Particles made up with grains and grains made up with crystallites) Crystal size measured in XRD and grain size and particle size in, SEM AFM. The crystal size does not exceed 10 nm. And the size of the grains did not exceed 60 nm, but the size of the particles was less than 100 nm [31,32]

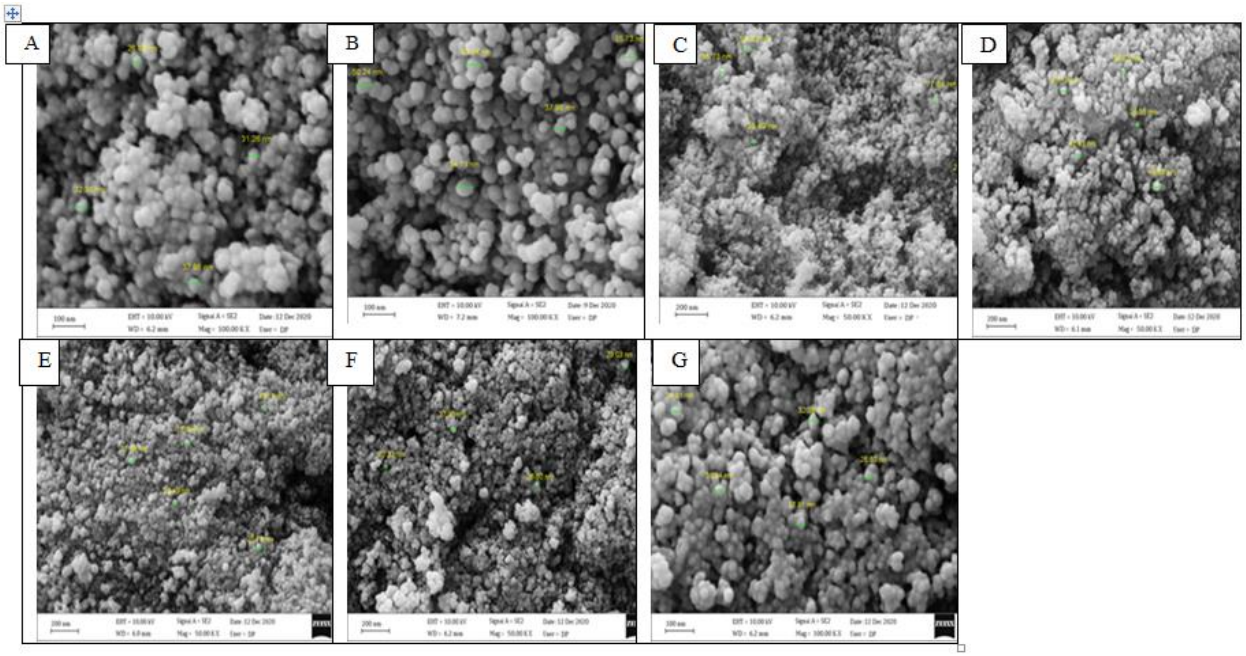

Figure .2 SEM images of (a) pure SnO_2 (b) doped witho.5% Cu (c) doped with1% Cu (d) doped with1.5% Cu (e)doped with2% Cu (f) doped with2.5% Cu (g) doped with 3% Cu.

EDX describes the composition of the elements in the prepared samples and that the copper ions have been successfully incorporated into the SnO_2 lattice, The EDX results are shown in Fig.3 which shows the rising peaks of Sn, O, Cu. The actual composition of the rated EDX prepared materials is scheduled in

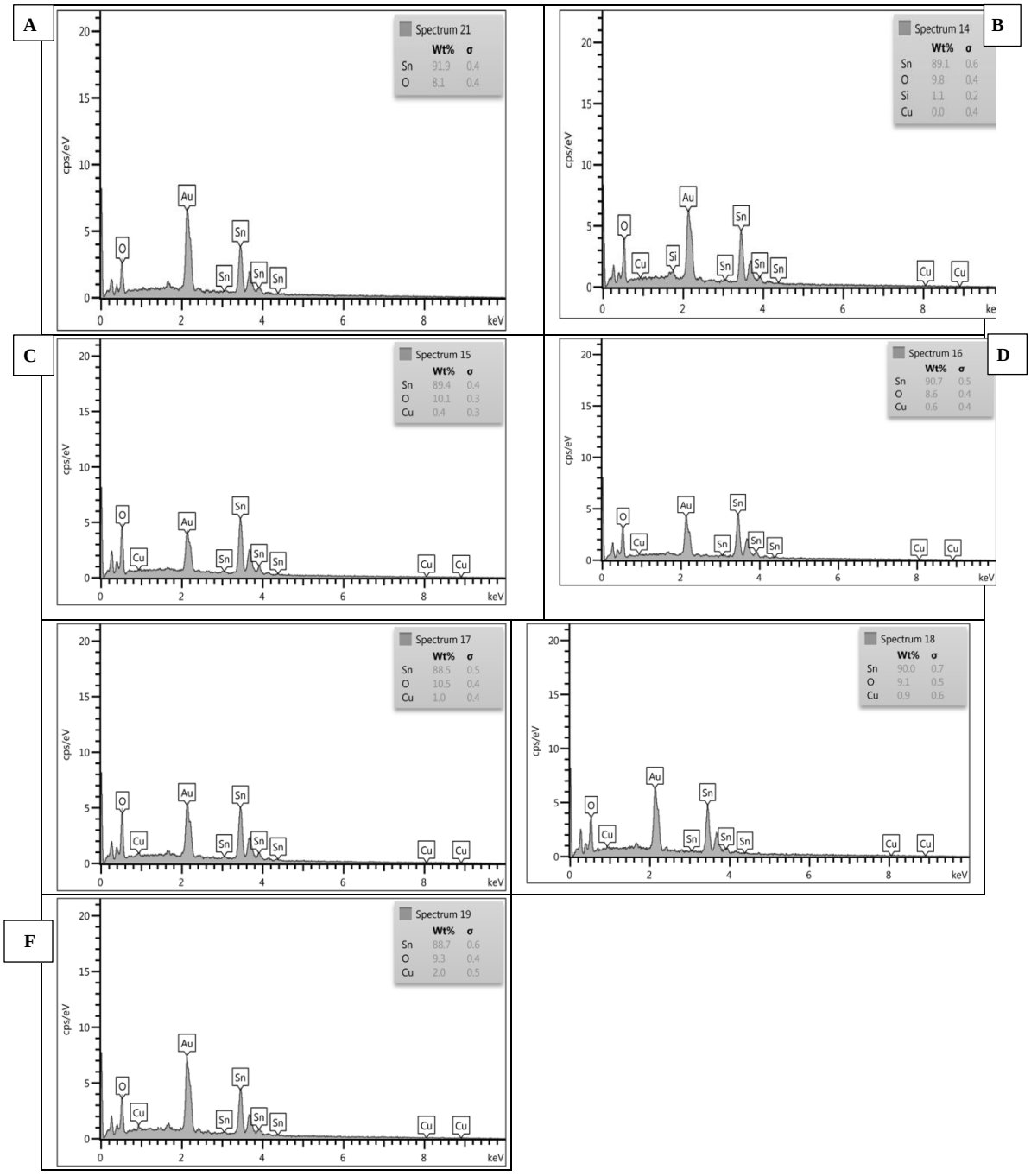

Figure .3 A) EDX image of pure SnO_2. B) doped with o.5% Cu. C) doped with 1% Cu. D) doped with 1.5% Cu. E) doped with 2% Cu. F) doped with 2.5% Cu. G) doped with 3% Cu.

Table 3. The actual composition of the rated EDX prepared materials is scheduled

EDX composition	Sn(wt%)	O(wt%)	Cu(wt%)
Pure	91.9	8.1	-
0.5%Cu	89.1	9.8	0
1%Cu	89.4	10.1	0.4
1.5%Cu	90.7	8.6	0.6
2%Cu	88.5	10.5	1
2.5%Cu	90	9.1	0.9
3%Cu	88.7	9.3	2

Optical studies

In order to better understand the effect of copper doping on the optical properties of SnO_2 nanoparticles at different concentrations. This UV-VIS Spectroscopy analysis was performed. Fig.4 shows the variation in absorbance with wavelength within the range of 280 nm-900 nm(The energy gap was within this range) for the pure SnO_2 samples and doped with Cu ions where the band gap is calculated using the Planck eq.4[33]:

$$E=\frac{1240}{\lambda}\ (ev)\ \ldots\ldots\ldots\ldots 4$$

The energy gap for pure SnO_2 nanoparticles doped with concentrations (0.5, 1, 1.5, 2, 2.5, and 3)

%wt of Cu are illustrated in Table 4. which shows how the energy gap value increases with increasing concentration Cu and decreases with increasing wavelength.The results match those of the researchers Saikia et al. [34]due to blue shifts as a result of the quantum confinement effect Sharma et al. [35], Vayssieres et al.[36] . It can be seen from Tab.4 below that the bandgap in pure is 4.33 ev and when copper doped decreased to 4.18 ev. The reason is due to the fact that the radius of the Cu +2 impurity ion is equal to 0.73Å when compared with the radius of the material Sn + 4 approaches 0.69A°, and this leads to the entry of copper impurities into the crystal of SnO2 in the form of an alternating impurity. When doping Cu by 0.5%, we notice that the energy gap decreased to 4.18 ev due to the formation of localized levels, but with the increase of doping, the band gap increased because the doping system is destroyed and works to destroy the lattice levels and thus increase the band gap and lead to an increase in oxygen vacancies and reduce the concentration of free electrons. The confinement of electrons and holes increases the band gap. and it all depends on where the Fermi level of doping is located, which causes tape tails to appear. As a result, the band gap effectively decreases or increases [37] SnO_2 n-type. after doping, band gap will increase because of rise number of majority carriers

Table 4. the energy band gap for pure Sno_2 nanoparticles doped with concentrations (0.5, 1, 1.5, 2, 2.5, and 3) %wt of Cu.

Concentration Cu ratios%	Band gap (Eg) ev	wave length (λ)nm
0	4.33	286
0.5	4.18	296
1	4.21	294
1.5	4.21	294
2	4.23	293
2.5	4.35	285
3	4.35	285

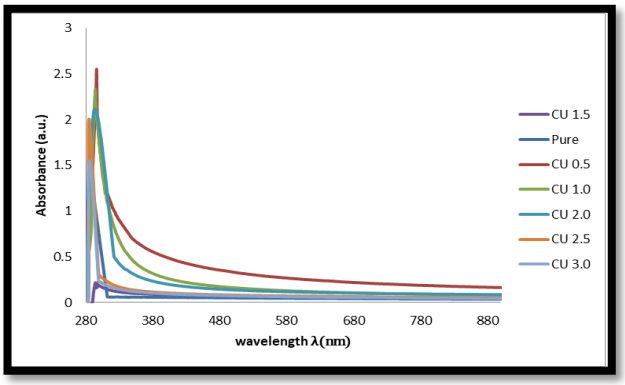

Figure.4 Shows the absorbance spectrum of pure Sno_2 NPs doped with Cu.

AFM examination

Fig.5 shows an atomic force microscope image of the pure SnO_2 sample surface and doped with Cu at different concentrations and annealed at 550 ° C, in 2D and 3D directions, to calculate the average surface roughness and average particle size as shown in Tab.5 below , i.e. the increase and decrease in the roughness rate and the average size pure SnO_2 nanoparticles and doped with Cu , From the Table 5, it can be noticed that the roughness is not related to the size of the grains, but from Fig. 5. the cumulative report explains this, as when the difference between the particle sizes is large, the roughness is greater, as is evident at 2%, although the average size was less, but higher roughness. Crystalline size is smaller than grain or particle size. inside a grain or particle, we have many crystals of identical orientation. Particle size and grain size are not same. one particle can have several grains [38]

Table 5. Shows the average size and roughness of pure SnO_2 nanopartical and doped with different concentration of Cu .

Cu doping concentration W%	average size (nm)	Roughness (nm)
0	98.9	3.04
0.5	72.56	25
1	92.91	27
1.5	88.38	16
2	76.79	41.8
2.5	70.94	23.6
3	71.21	25.2

From Tab.5, we note that the best roughness is at the concentration of copper 2%, and this indicates that this percentage is the best in medical applications.

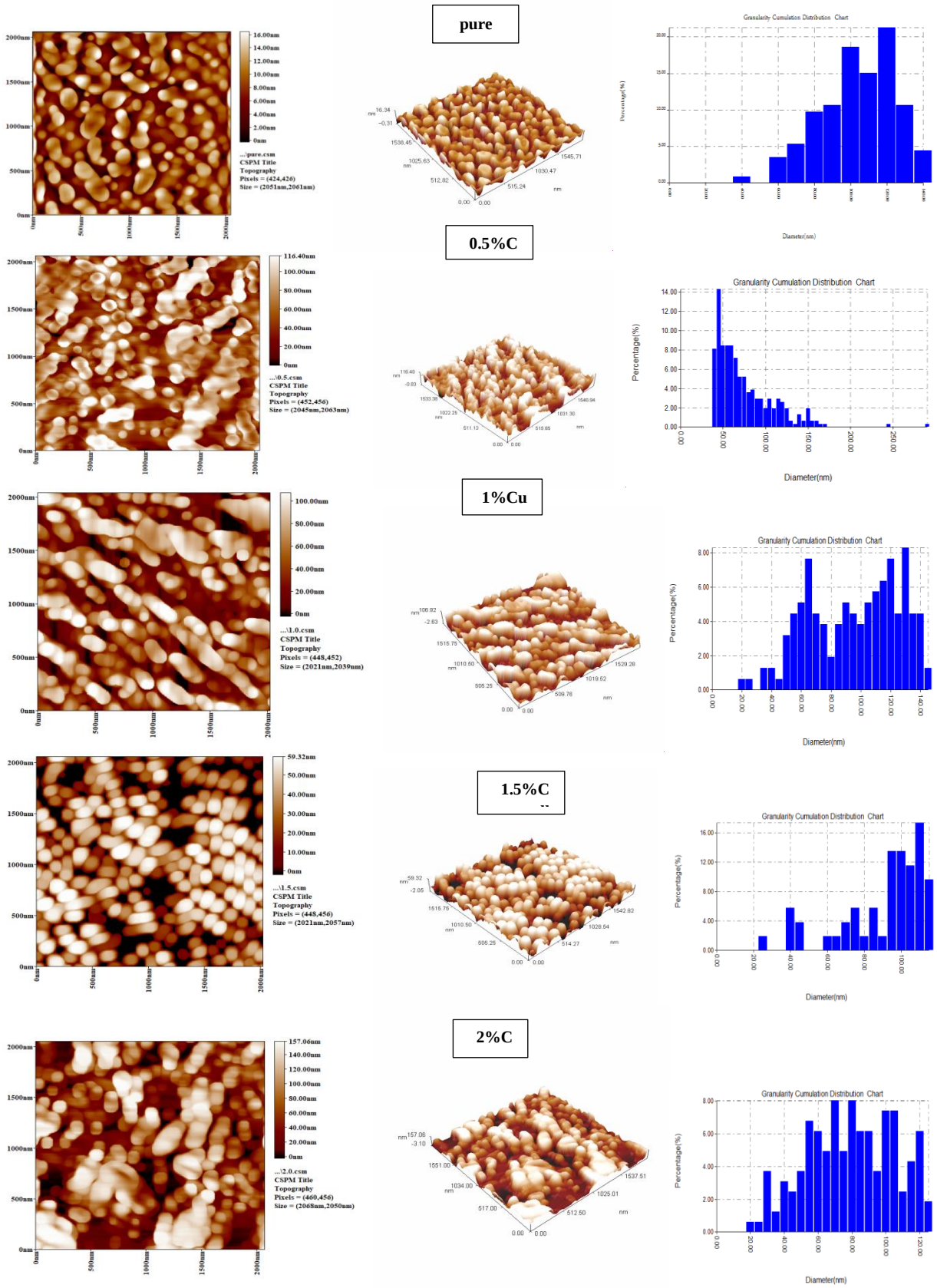
pure
0.5%C
1%Cu
1.5%C
2%C
Granularity Cumulation Distribution Chart
Percentage(%)
Diameter(nm)

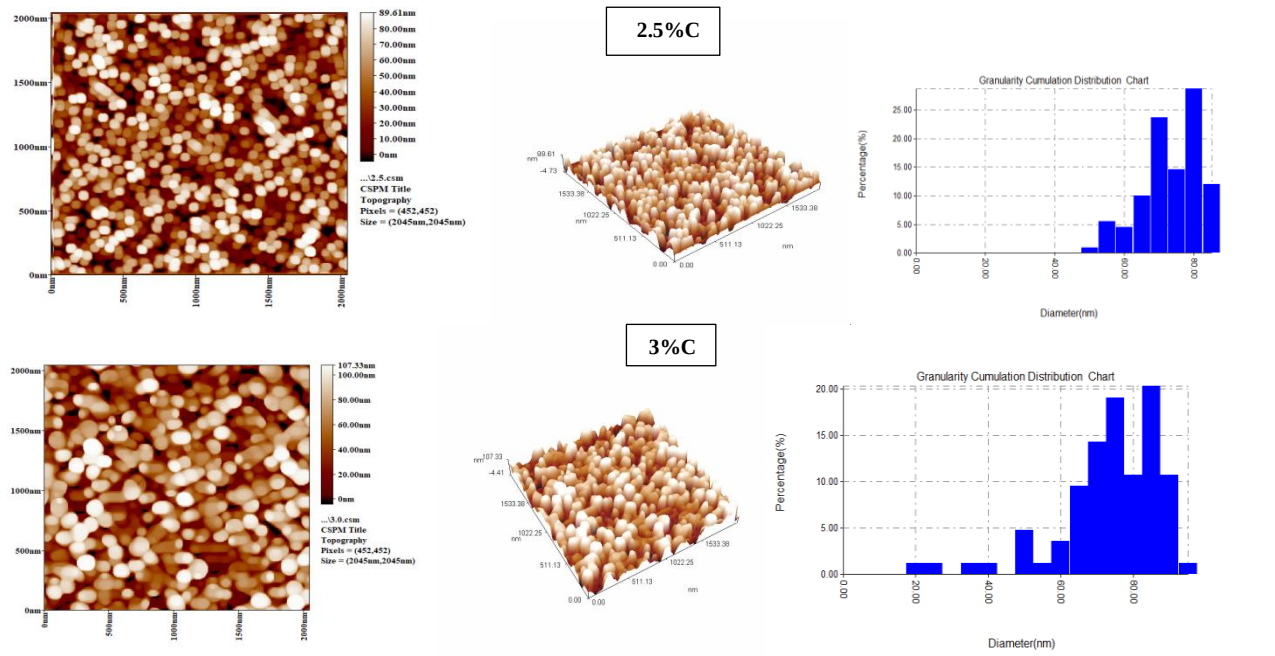

Figure 5. The AFM of pure SnO_2 nanoparticles and doped with different concentration of Cu in 2D, 3D of Granularity Cumulation Distribution Repor.

Authors' declaration:

- Conflicts of Interest: None.
- We hereby confirm that all the Figures and Tables in the manuscript are mine ours. Besides, the Figures and images, which are not mine ours, have been given the permission for re-publication attached with the manuscript.
- Ethical Clearance: The project was approved by the local ethical committee in University of Baghdad.

Conclusion:

In this paper, pure tin oxide nanoparticles have been synthesized and doped with copper by chemical precipitation method, this method is simple and effective to form Tin oxide nanoparticles. The compositions of the pure tin oxide nanoparticles and doped with different concentration of Cu are characterized by XRD, SEM, AFM and UV -VIS Spectrometer. The XRD pattern shows that the Tin oxide nanoparticles formed from this synthesis are tetragonal polycrystalline and that the crystal size is (9.97,8.35,8.36,8.67, 9,7, and8.86) nm for pure samples and doped with (0.5,1,1.5,2,2.5, and 3) wt% of Cu. The results of the AFM show that the grain size within the nanoscale, are spherical in shape with different sizes ranging from (98.9 ,72.5, 92.9 ,88.3 ,76.7 ,70.9,71.2) nm. The higher roughness is 41.8 nm for sample doped with 2%Cu. The roughness of pure samples is 3.04 nm. The uv-vis spectroscopy results show that the energy gap increases with increasing doping. From the results obtained, it is evident that the prepared samples can be used in various electronic applications, such as using them as a gas sensor as well as in various medical applications such as cancer.

Authors' contributions statement:

Nada K. Abass conceived of the presented idea. Duha S. Shaker* developed the theory and performed the computations. and verified the analytical methods. Nada K. Abass and Ruqayah A. Ulwall encouraged Duha S. Shaker*. to investigate [a specific aspect] and supervised the findings of this work. All authors discussed the results and contributed to the final manuscript

References:

1. Hornyak GL, Moore JJ, Tibbals HF, Dutta J. Fundamentals of nanotechnology. 1St ed. Boca Raton: Taylor&Francis Group ; 2009. Ch.1, P .786-4.
2. Poole Jr CP, Owens FJ. Introduction to nanotechnology.1St ed.Hoboken,New Jersey,in Canada : John Wiley & Sons,Inc;2003. Ch.1, P.388-4.
3. Pascariu P, Airinei A, Grigoras M, Fifere N, Sacarescu L, Lupu N, et al. Structural, optical and magnetic properties of Ni doped SnO_2 nanoparticles. J. Alloys Compd. 2016; 668:65–72.
4. Dey A. Semiconductor metal oxide gas sensors: A review. Mat Sci Eng B-Adv. 2018; 229:206– 17.
5. Mubeenabanu A, Veemaraj T. Effect of Ag Doping on Structural and Optical Properties of ZnO Nanoparticles. Adv Appl Sci Res. 2017;1(9).
6. Gautam S, Agrawal H, Thakur M, Akbari A, Sharda H, Kaur R, et al. Metal oxides and metal organic frameworks for the photocatalytic degradation: A review. J. Environ. Chem. Eng.. 2020;8(3):103726.

7. Danish MSS, Estrella LL, Alemaida IMA, Lisin A, Moiseev N, Ahmadi M, et al. Photocatalytic Applications of Metal Oxides for Sustainable Environmental Remediation. Metals 2021, 11, 80. MDPI; 2021.
8. Umar A, Ammar HY, Kumar R, Almas T, Ibrahim AA, AlAssiri MS, et al. Efficient H2 gas sensor based on 2D SnO_2 disks: experimental and theoretical studies. Int. J Hydrog Energ. 2020;45(50):26388–401.
9. Pascariu P, Airinei A, Olaru N, Petrila I, Nica V, Sacarescu L, et al. Microstructure, electrical and humidity sensor properties of electrospun NiO–SnO_2 nanofibers. Sens. Actuators B Chem. 2016; 222:1024–31.
10. Sharma N, Jha R, Jindal N. Hydrothermally Synthesized Stannic Oxide Nano-hexagons. Mater Today Proc. 2018;5(5):13807–15.
11. Periyasamy M, Kar A. Modulating the properties of SnO_2 nanocrystals: morphological effects on structural, photoluminescence, photocatalytic, electrochemical and gas sensing properties. J. Mater Chem C. 2020;8(14):4604–35.
12. Mehra S, Bishnoi S, Jaiswal A, Jagadeeswararao M, Srivastava AK, Sharma SN, et al. A review on spectral converting nanomaterials as a photoanode layer in dye-sensitized solar cells with implementation in energy storage devices. Energy Storage Mater. 2020;2(2):e120.
13. Xu R, Zhang L-X, Li M-W, Yin Y-Y, Yin J, Zhu M-Y, et al. Ultrathin SnO_2 nanosheets with dominant high-energy {001} facets for low temperature formaldehyde gas sensor. Sens. Actuators B Chem. 2019; 289:186–94.
14. Kadhim IH, Hassan HA, Ibrahim FT. Hydrogen gas sensing based on nanocrystalline SnO2 thin films operating at low temperatures. Int J Hydrogen Energ. 2020;45(46):25599–607.
15. Kadhim IH, Hassan HA. Hydrogen gas sensing based on SnO_2 nanostructure prepared by sol–gel spin coating method. J Electron Mater. 2017;46(3):1419–26.
16. Chithra MJ, Sathya M, Pushpanathan K. Effect of pH on crystal size and photoluminescence property of ZnO nanoparticles prepared by chemical precipitation method. Acta Metal Sin Eng llett. 2015;28(3):394–404. 2015;28(3):394–404.
17. Amendola V, Amans ID, Ishikawa Y, Koshizaki N, Scirè S, Compagnini G, et al. Room-Temperature Laser Synthesis in Liquid of Oxide, Metal-Oxide Core-Shells, and Doped Oxide Nanoparticles. Chemistry. 2020;26(42):9206.
18. Khan D, Rehman A, Rafiq MZ, Khan AM, Ali M. Improving the Optical properties of SnO_2 nanoparticles through Ni doping by sol-gel Technique. CRGSC. 2021;100079.
19. Nada A, Khalid R, Zainb J. New Method of Preparation ZnS Nano size at low pH. Int. J. Electrochem. Sci., 2013;(8): 3049 - 3056
20. Vojvodić K, Nikolić-Bujanović L, Mrazovac-Kurilić S, Staletović N. Application of ecofrendly oxidant ferrate (vi) in the metallurgical processes of copper extraction. J. Min. Metall., Sect. B Metall. 2018;(3–4):97–108.
21. Nada A, Mohammed T, Lamia A," Fabricated of Cu Doped ZnO Nanoparticles for Solar Cell Application" Baghdad Sci. J. 2018;15(2).
22. Mohammed A, Bachtiar D, Siregar JP, Rejab MRM. Effect of sodium hydroxide on the tensile properties of sugar palm fibre reinforced thermoplastic polyurethane composites. J Mech Eng. Sci. 2016;10(1):1765–77.
23. Muliyadi L, Doyan A, Susilawati S, Hakim S. Synthesis of SnO_2 Thin Layer with a Doping Fluorine by Sol-Gel Spin Coating Method. J JPPIPA. 2019;5(2):175–8.
24. Sagadevan S, Johan M, Bin R, Aziz FA, Hsu H-L, Selvin R, et al. Influence of Mn Doping on the Properties of Tin Oxide Nanoparticles Prepared by Co-Precipitation Method. J Nanoelectron. Optoelectron. 2019;14(4):583–92.
25. Yakout SM. Robust ferromagnetic and fast sunlight photocatalytic properties of nanocrystalline SnO_2: Co/Cu codoping. Ceram. Int. 2021;47(7):10104–12.
26. Ehsani M, Hamidon MN, Toudeshki A, Abadi MHS, Rezaeian S. CO_2 gas sensing properties of screen-printed La_2O_3/SnO_2 thick film. IEEE Sens J. 2016;16(18):6839–45.
27. Mason RP, Tulenko TN, Jacob RF. Direct evidence for cholesterol crystalline domains in biological membranes: role in human pathobiology. Biochim Biophys Acta, Biomembr. 2003;1610(2):198–207.
28. Sarmah S, Kumar A. Electrical and optical studies in polyaniline nanofibre–SnO_2 nanocomposites. Bull Mater Sci. 2013;36(1):31–6.
29. Gosens I, Post JA, de la Fonteyne LJJ, Jansen EHJM, Geus JW, Cassee FR, et al. Impact of agglomeration state of nano-and submicron sized gold particles on pulmonary inflammation. Part Fibre Toxicol. 2010;7(1):1–11.
30. Dahman Y. Nanotechnology and functional materials for engineers. 1St ed . Elsevier; 2017. Ch.1, An Introduction to Nanotechnology; P .282-14.
31. Iwashita N. X-ray powder diffraction. In: Materials science and engineering of carbon.1St ed. Elsevier; 2016.; p. 7–25.
32. Andrade AB, Ferreira NS, Valerio MEG. Particle size effects on structural and optical properties of BaF 2 nanoparticles. RSC Adv. 2017;7(43):26839–48.
33. Shamaila S, Bano T, Sajjad AKL. Efficient visible light magnetic modified iron oxide photocatalysts. Ceram Int. 2017;43(17):14672–7.
34. Saikia K, Deb P, Kalita E. Sensitive fluorescence response of ZnSe (S) quantum dots: an efficient fluorescence probe. Phys Scr. 2013;87(6):65802.
35. Sharma RK, Agrawal M, Marshall F. Heavy metal contamination in vegetables grown in wastewater irrigated areas of Varanasi, India. Bull Environ Contam Toxicol. 2006;77(2):312–8.
36. Vayssieres L, Sathe C, Butorin SM, Shuh DK, Nordgren J, Guo J. One-dimensional quantum-confinement effect in α-Fe_2O_3 ultrafine nanorod arrays. Adv. Mater. 2005;17(19):2320–3.

37. Ziabari AA, Ghodsi FE. Influence of Cu doping and post-heat treatment on the microstructure, optical properties and photoluminescence features of sol–gel derived nanostructured CdS thin films. J Lumin. 2013; 141:121–9.

38. Brindley GW. XLV. The effect of grain or particle Size on X-ray reflections from mixed powders and alloys, considered in relation to the quantitative determination of crystalline substances by X-ray methods. Mater Sic. 1945;36(256):347–69.

تحضير ودراسة الخصائص الهيكلية، الشكلية والبصرية لجسيمات نانوية من اوكسيد القصديرالنقي ومخدرCu

ضحى سعد شاكر **ندى خضير عباس** **رقية عبد الولي عبد الله**

قسم الفيزياء، كلية العلوم للبنات، جامعة بغداد، بغداد، العراق.

الخلاصة:

في هذه الدراسة، تم تصنيع جزيئات SnO_2 النانويه النقيه والمشوبة بالنحاس بواسطة طريقه الترسيب الكيميائي . تم استخدام $SnCl_2.2H_2O$ ، $CuCl_2.2H_2O$ كمواد خام . تم تلدين المواد عند 550 °C لمدة 3ساعات من اجل تحسين التبلور. اظهرت نتائج حيود الاشعه السينية ان العينات تبلورت في طورمن نوع رباعي الروتيل SnO_2 , نظرا ان متوسط الحجم البلوري ل SnO_2النقي 9 نانومتر ويختلف مع تغير منشطات النحاس (0.5%, 1%, 1.5%, 2%, 2.5%, 3%)، ، (8.86, 9,7 , 8.67, 8.36, 8.35) نانومتر على التوالي والتركيب البلوري SnO_2 لا يتغير مع ادخال النحاس ، أكدت نتائج SEM للنقاوة والمخدر أن حجم الجسيمات يقع في نطاق (25-56) نانومتر داخل الحجم النانوي .كانت دراسات UV-ViS حيث كشف التحليل الطيفي للانعكاس ان طاقه فجوة النطاق تزداد مع زيادة نسب المنشطات (4.18,4.33، 4.21 ، 4.21 4.35,4.23) الكترون فولت للنقي والمشوب بالنحاس ((0.5%, 1%, 1.5%, 2%, 2.5%, 3%) على توالي . واظهرت نتائج AFMمعدل الخشونة،SPM وحجم الحبوب للعينات النقيه والمشوبة وان معدل الخشونة نانومتر و (3.04, 25,27,16,41.8,23.6,25.2) ومعدل القطر (71.21, 70.94, 76.79, 88.38, 72.56,92.91, 98.9) نانومتر للنقي والمشوب على التوالي.

الكلمات المفتاحية: جزيئات SnO_2 النانوية المخدر ب Cu، طريقة الترسيب الكيميائي ، UVومحلل حجم الجسيمات ، SEM، اوكسيد القصدير .